Liquid Crystals
Publication details, including instructions for authors and subscription information:
http://www.informaworld.com/smpp/title~content=t713926090

The case of missing incommensurate smectic A phases

Prem Patel[a]; Satyendra Kumar[a]; Paul Ukleja[b]
[a] Department of Physics, Liquid Crystal Institute, Kent State University, Kent, Ohio, U.S.A. [b] Department of Physics, University of Massachusetts at Dartmouth, North Dartmouth, Massachusetts, U.S.A.

To cite this Article Patel, Prem , Kumar, Satyendra and Ukleja, Paul(1994) 'The case of missing incommensurate smectic A phases', Liquid Crystals, 16: 3, 351 — 371
To link to this Article: DOI: 10.1080/02678299408029161
URL: http://dx.doi.org/10.1080/02678299408029161

LIQUID CRYSTALS, 1994, VOL. 16, NO. 3, 351–371

Invited Article

The case of missing incommensurate smectic A phases

by PREM PATEL and SATYENDRA KUMAR*
Department of Physics and Liquid Crystal Institute,
Kent State University, Kent, Ohio, 44242-0001, U.S.A.

and PAUL UKLEJA
Department of Physics, University of Massachusetts at Dartmouth,
North Dartmouth, Massachusetts, 02747, U.S.A.

(*Received 3 June 1993; accepted 16 July 1993*)

Two binary mixtures of polar liquid crystal materials were previously reported to exhibit three incommensurate smectic A phases predicted for such materials on the basis of phenomenological theory. Results of our recent high-resolution X-ray scattering experiments show that no incommensurate phases exist in the two systems. Wide coexistence regions are found at first order transitions between various frustrated smectic phases of these mixtures. These regions were previously identified as the incommensurate smectic A phases. The phase diagrams of the two systems determined with high-resolution X-ray technique are shown to be in excellent agreement with Barois–Prost–Lubensky theory.

1. Introduction

The smectic A (S_A) phase is characterized by long-range translational order in one dimension and liquid-like arrangement of anisotropic organic molecules in the other two dimensions. Only one type of S_A phase was known until 1979, when a transition from one S_A phase to another was observed [1]. This discovery marked the beginning of a new subfield of liquid crystals now known as the *frustrated* or *polar* smectics. The existence of more than nine frustrated smectic phases and multiple reentrance of nematic and smectic phases are now well established [2].

The molecules that exhibit frustrated smectic phases have a permanent terminal dipole and a long aromatic core usually made of three benzene rings. Four representative molecules relevant to discussions in this paper are shown in figure 1. These molecules have a natural tendency to form dimer-like pairs which plays a key role in determining their mesomorphism. Microscopic molecular arrangements in several frustrated phases and their characteristic X-ray diffraction patterns are shown in figure 2. Here, the molecules are drawn as straight lines and their dipoles as arrowheads at one end. At a high temperature, the molecules are oriented *on average* parallel to the *director*, $\hat{\mathbf{n}}$, in the nematic phase. Because of the two length scales, which correspond to the molecular and dimer lengths, two diffuse rings are observed in the X-ray diffraction pattern of the polar nematic phase.

* Author for correspondence.

0267–8292/94 $10·00

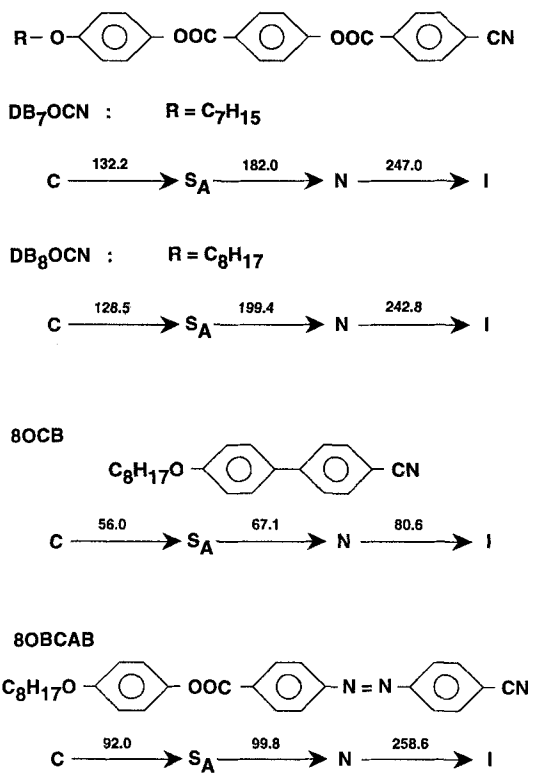

Figure 1. Molecular formulae of the DB*n*OCN series, 8OCB, and 8OBCAB. The phases exhibited and the transition temperatures (°C) are also shown.

The smectic A_1 phase forms when the molecules develop a one-dimensional density modulation parallel to the director. In this phase, the molecular dipoles point up and down with equal probability. The density modulation gives rise to a quasi-Bragg reflection and the dimers (weakly associated nearest neighbours) are responsible for the diffuse peak centred at a different and, in general, incommensurate value of the scattering vector. The majority of the dipoles point up in one smectic layer and down in the adjacent one to form the smectic A_2 phase. The molecular dipoles in this phase possess antiferroelectric ordering at alternating smectic layer interfaces and develop a second (dipole density) modulation of period that is twice the molecular length. However, if the molecules partially overlap in the longitudinal direction then the two modulation lengths are smaller than the molecular length and the smectic phase formed is known as the S_{A_d} phase. These phases can be thought of, as first proposed by Barois [3], as having two density modulations. The two modulations are evidently collinear with $\hat{\mathbf{n}}$ in the S_{A_1}, S_{A_d}, and S_{A_2} phases. However, there are several phases, such as $S_{\tilde{A}}$, $S_{A_{\text{crenellated}}}$, etc., in which the two modulations are not collinear.

2. Theoretical background

Prost, Lubensky, and co-workers [3–7] developed a very successful phenomenological description of these systems using two 2-component order parameters Ψ_1 and Ψ_2,

$$\Psi_i = \Psi_{i0} \exp[i(\mathbf{q}_i \cdot \mathbf{r})]; \quad i = 1,2$$

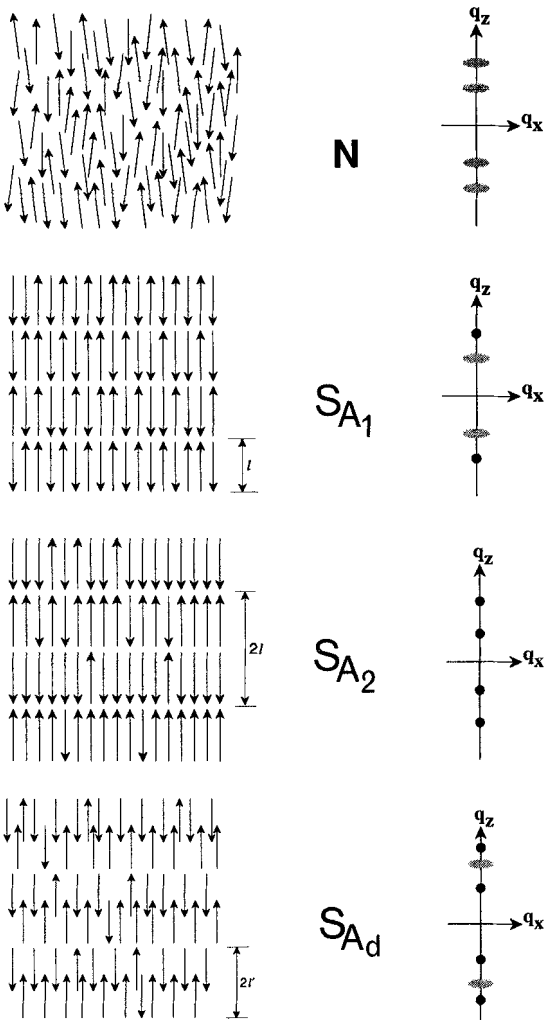

Figure 2. Schematic representations of the polar nematic and three frustrated smectic A phases with their characteristic diffraction patterns. The molecules are drawn as thin rods with arrows on one end to denote the longitudinal dipoles. Here, l is the molecular length and $2l'$ ($l < 2l' < 2l$) is the effective length of the dimer-like molecular arrangement formed in the S_{A_d} phase. The smectic layer spacings of the various phases are shown in terms of l and l'. The dots represent quasi-Bragg reflections, while the diffuse peaks represented by ellipses arise from short-range ordering of molecules or dimers.

that characterize long-range head to head antiferroelectric order and the smectic mass density modulation, respectively. The wave vectors $\mathbf{q}_1$ and $\mathbf{q}_2$ are in general not collinear. The two order parameters would prefer to condense at their natural magnitudes k_1 $(=2\pi/2l')$ and k_2 $(=2\pi/l)$, respectively, in the absence of coupling between them. Here, l, $2l'$ $(\leqslant 2l)$ are the molecular length and the effective length of an antiferroelectrically ordered pair of molecules, respectively. The excess free energy density can be written as

$$\begin{aligned} f-f_0 = {} & a_1(T-T_{1c})|\Psi_1|^2 + D_1|(\Delta+k_1^2)\Psi_1|^2 + C_1|\nabla_\perp\Psi_1|^2 + u_1|\Psi_1|^4 \\ & + a_2(T-T_{2c})|\Psi_2|^2 + D_2|(\Delta+k_2^2)\Psi_2|^2 + C_2|\nabla_\perp\Psi_2|^2 + u_2|\Psi_2|^4 \\ & + 2u_{12}|\Psi_1|^2|\Psi_2|^2 - w\,\mathrm{Re}\,\Psi_1^2\Psi_2^* - v\,\mathrm{Re}\,\Psi_1\Psi_2^*. \end{aligned}$$

Here T_{ic} are the two mean field transition temperatures. The elastic terms with coefficients D_i describe the spatial modulations and favour $q_1^2 = k_1^2$ and $q_2^2 = k_2^2$. Terms with $\nabla_\perp$, a gradient in the plane perpendicular to $\hat{\mathbf{n}}$, favour that $\mathbf{q}_1$ and $\mathbf{q}_2$ both be parallel to $\hat{\mathbf{n}}$. The terms $\Psi_1\Psi_2^*$ and $\Psi_1^2\Psi_2^*$ favour lock-in of two wavevectors at $\mathbf{q}_1 = \mathbf{q}_2$ and $\mathbf{q}_1 = \mathbf{q}_2/2$, respectively. These competing tendencies give rise to a variety of phases in mixtures of compounds with very different molecular length. In such binary mixtures, the quantities Ψ_1 and Ψ_2 depend on concentration, which influences the strength of the coupling terms and the natural wavevectors. The cubic term dominates when $l' \sim l$, but the harmonic term becomes most important when $l' \sim l/2$.

The formation of various smectic phases follows quite naturally from this theory. When $\Psi_1 = \Psi_2 = 0$, a nematic phase is obtained which possesses neither a mass density nor a polarization density modulation. In the monolayer S_{A_1} phase, only the mass density wave develops, so $\Psi_1 = 0$ and $\Psi_2 \neq 0$. The quasi-Bragg reflection from this phase appears at $2q_0 = 2\pi/l$. Several interesting cases arise when $\Psi_1 \neq 0 \neq \Psi_2$. If both density waves are collinear and $l' \cong l$, then the cubic coupling term enforces commensurability, requiring $q_2 = 2q_1 = 2\pi/2l$ $(= q_0$, say) and the bilayer S_{A_2} phase results. On the other hand, if $l' < l$, as will be the case if molecules were overlapping, then the partial bilayer phase, S_{A_d}, is obtained. Obviously, this theory provides a satisfactory explanation of the smectic polymorphism in these materials.

3. The incommensurate smectic A phases

If the ratio k_2/k_1 cannot be expressed as a ratio of two integers, then the two density waves may simultaneously condense to form *incommensurate* smectic phases [8–10]. These phases are likely to be stable when the coefficient C_1 of the gradient term, which constrains the wavevector $\mathbf{k}_1$ to be parallel to the director and ensures collinearity of $\mathbf{k}_1$ and $\mathbf{k}_2$, and the mismatch between the natural wavevectors $(k_1^2 - k_2^2/4)$ are large. Modulated structures with solitons are formed when coupling between order parameters is strong. In this $S_{A_{is}}$ phase, the two modulations remain out of phase in soliton regions which separate the phase-locked regions, as shown in figure 3. Three strong quasi-Bragg reflections at $2q_0$, q'', and $q_s = (2q_0 - q'')$ are expected in X-ray diffraction from this phase. Other reflections at q-values that are higher harmonics of $2q_0$ and q'', as well as their sums and differences, should also be present although their intensities may not be experimentally observable. The periodicity $Z = 2\pi/(q'' - q_s)$ of discommensurations in the $S_{A_{is}}$ phase is expected to diverge at the transition to the commensurate S_{A_2} phase.

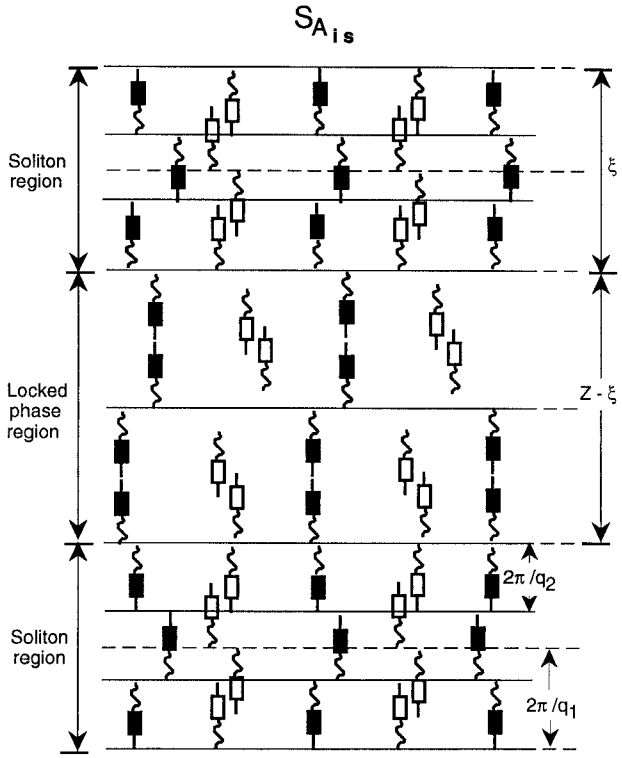

Figure 3. Real space representation of the incommensurate soliton $S_{A_{is}}$ phase. The central rigid part of the molecules is represented by a rectangle, the aliphatic tail by a wavy line and the dipoles by short straight lines on one end of the rectangle. In this phase, regions of width ξ with two independent wave-vectors k_1 and k_2, separate regions of width $Z-\xi$ in which the two modulations are phase-locked. The molecules form dimer-like arrangements with no overlap (dark rectangles) or with lengthwise partial overlap (white rectangles) and define periodic structures of incommensurate modulations. The dark and white molecules do not represent chemically different species.

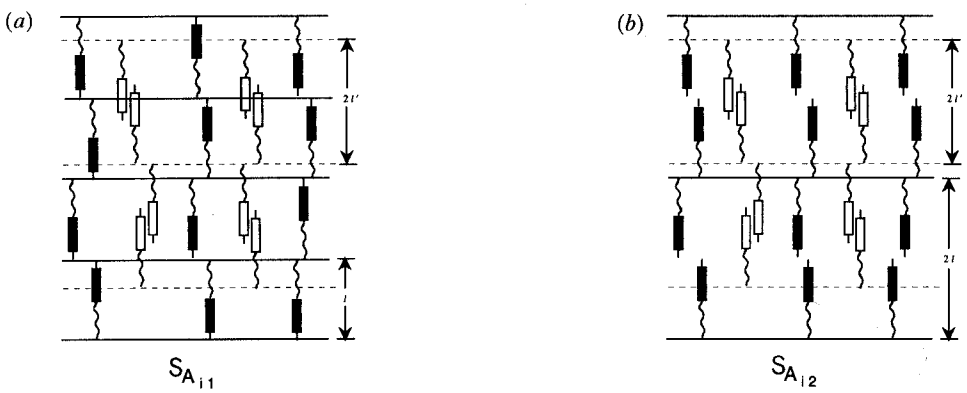

Figure 4. Real space representation of the incommensurate $S_{A_{ic}}$ phases. (*a*) In the $S_{A_{i1}}$ phase, two interpenetrating smectic modulations, with periodicities of l (dark molecules) and $2l'$ (open molecules) with overlapping dimer-like arrangements, coexist. (*b*) The $S_{A_{i2}}$ phase consists of S_{A_d} like (open molecules) and S_{A_2} like (dark molecules) molecular arrangements.

Weak coupling between the two order parameters allows the two periodic modulations to be simultaneously present. Although not a rigorous representation, two possible molecular arrangements in the weakly coupled $S_{A_{1c}}$ phase are shown in figure 4. The X-ray diffraction pattern of the $S_{A_{1c}}$ phase should consist of strongest reflections at q' and q_0 (or $2q_0$).

4. Discovery of the incommensurate phases

First evidence of incommensurate smectic modulations was provided [11] by Brownsey and Leadbetter in 1980 in the smectic E phase of a cyano compound 4-octyl-4″-cyano-*p*-terphenyl (T24). In 1985, the presence of an incommensurate phase was reported [12] in binary mixtures of 4-octyloxy-4′-cyano-biphenyl (8OCB) and 4-*n*-heptyloxyphenyl 4′-cyanobenzoyloxybenzoate (DB7OCN). Three quasi-Bragg peaks were observed in powder X-ray diffraction pattern of this phase. Two of the peaks were at incommensurate values of wavevectors, while the third one was a second harmonic of one of them. This phase was found for the 25 to 40 mol% concentration range of 8OCB as shown in figure 5(*a*). It was believed to be a modification of the $S_{A_{1c}}$ phase denoted by $S_{A_{i2}}$. This report engendered much interest [13, 14] in frustrated smectic

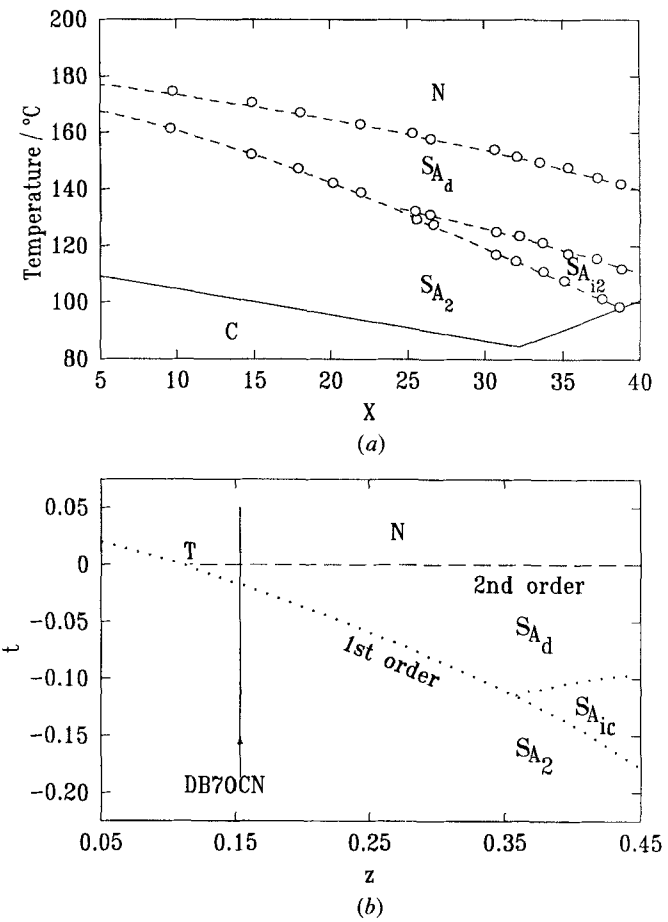

Figure 5. (*a*) Phase diagram of DB7OCN + 8OCB adapted from [12]. (*b*) Theoretical phase diagram (adapted from [15]) showing N–S_{A_d}–$S_{A_{1c}}$–S_{A_2} phases in the (t, z) plane. Here z is the incommensurability parameter that scales as the concentration of 8OCB.

materials. Prost's phenomenological model was generalized by Barois [15] and an incommensurate phase was found to be stable for a range of values of the incommensurability parameter z. The calculated phase diagram, figure 5 (*b*), was found to be fully compatible with experiments. The results of heat capacity, optical, and dielectric studies that followed supported the existence of a unique phase in the reported range of concentration and temperature in this system.

High-resolution X-ray scattering measurements [16] on a mixture of 77·12 mol% 4-cyano-4-[(4-pentylphenoxy)carbonyl]phenylester (DB5) and 22·88 mol% 4-octyloxy-4-[2-(4-cyanophenyl)ethenyl] phenyl ester (T8) revealed strong incommensurate density fluctuations between the S_{A_d} and S_{A_1} phases. Figure 6 shows the growth of diffuse peaks at [17] q_0' and $2q_0 - q_0'$ with decreasing temperature, suggesting the presence of incommensurate fluctuations. The intensity contour map in the *hk*-plane of the reciprocal space was in good qualitative agreement with that calculated from Wang–Lubensky [7] theory for an appropriate value of z. The estimated size of these correlations was only 200–300 Å or approximately ten smectic layers. These fluctuations evolved into smectic Ã fluctuations before they were pre-empted by a first order transition to the S_{A_2} phase.

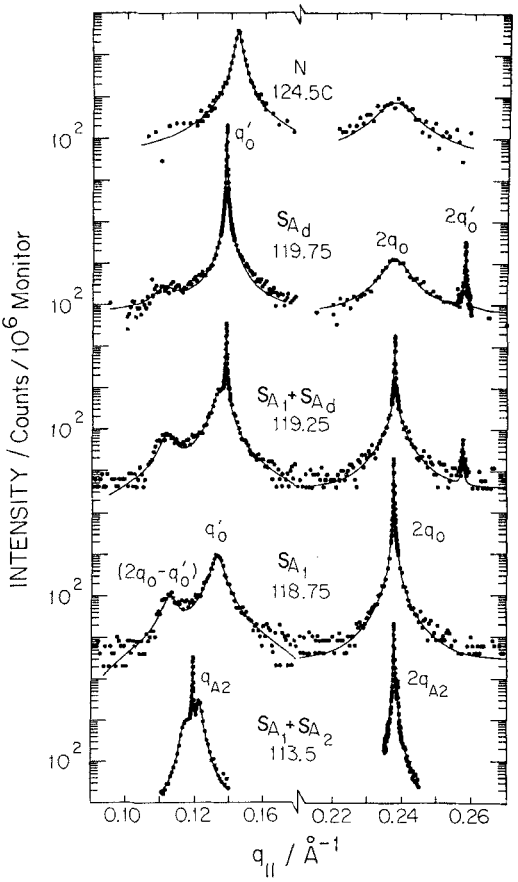

Figure 6. $q_{\parallel}$-scans (reproduced from [16]) at the indicated temperatures for a mixture of DB5 and T8. The presence of diffuse peaks [17] at q_0' and $2q_0 - q_0'$ at 118·75°C is due to incommensurate phase fluctuations. This modulation does not fully develop due to intervention by the first order transition to the S_{A_2} phase.

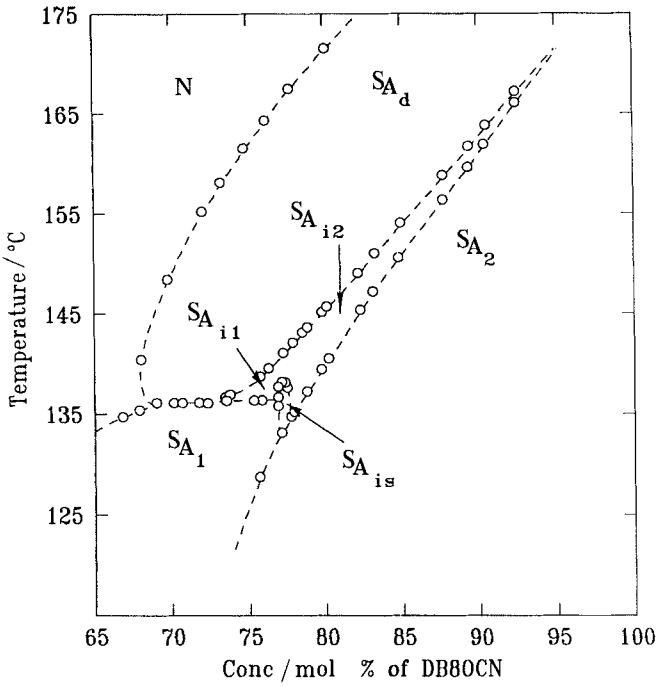

Figure 7. Partial phase diagram for binary mixtures of DB8OCN and 8OBCAB. The $S_{A_{i1}}$ and $S_{A_{i2}}$ phases were reported in addition to the soliton phase, A_{is} (adapted from [18]).

The data, which most strongly and quantitatively supported the existence of not only one but three incommensurate smectic phases, came from X-ray studies [18] of mixtures (figure 7) of 4-*n*-octyloxyphenyl 4′-cyanobenzoyloxybenzoate (DB8OCN) and 4-octyloxybenzoate-4′-cyanoazobenzene (8OBCAB) (more correctly named 4-octyloxyphenoxycarbonyl-4′-cyanoazobenzene). The results of previous X-ray experiments [18] are reproduced in figure 8. The smectic modulation wave vectors and their temperature dependence appeared to be in very good quantitative agreement with theoretical predictions. The periodicity Z of discommensurations diverged at the transition to the S_{A_2} phase, precisely as predicted by theory.

The accumulated experimental evidence discussed above appeared to confirm the existence of incommensurate phases in both weak and strong coupling limits. However, recent high-resolution X-ray diffraction experiments conducted at Kent State University show that all incommensurate phases discovered so far are indeed coexistence of two or more frustrated smectic phases. The correct phase diagrams of both systems determined with the high-resolution technique are in agreement with those originally predicted by Barois, Prost and Lubensky. In the following sections we first briefly describe the experimental technique and then discuss the results for the two binary mixtures.

5. High-resolution X-ray diffraction

High-resolution X-ray scattering experiments were carried out using an 18 kW Rigaku RU-300 rotating anode X-ray generator in conjunction with a two-circle Huber goniometer. Details of the experimental set-up can be found elsewhere [19–21]. The longitudinal resolution $\Delta q_{\|}$ obtained with the use of single germanium crystals as

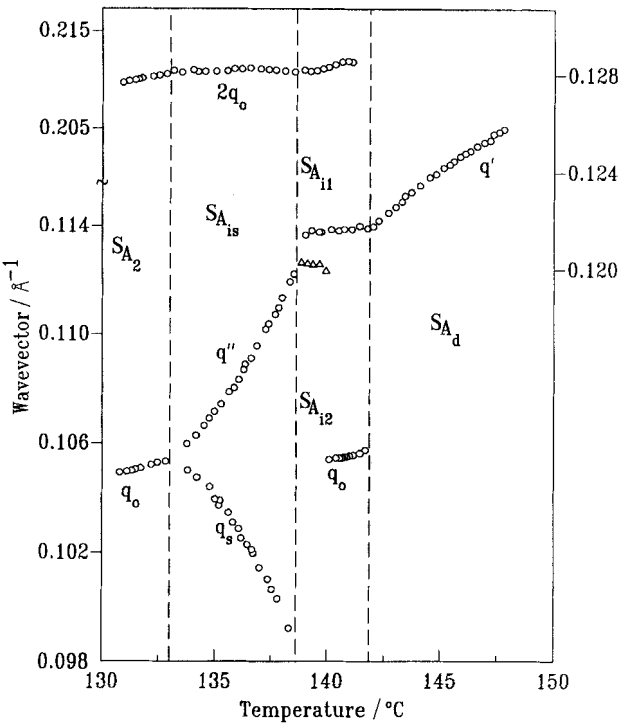

Figure 8. Temperature dependence of wave-vectors characterizing different smectic phases for the 77·2 mol per cent mixture of DB8OCN + 8OBCAB. Three sharp reflections at $2q_0$, q'' and $q_s = 2q_0 - q''$ are seen in the $S_{A_{is}}$ phases (adapted from [18]).

monochromator and analyser was measured to be 4×10^{-4} Å^{-1}, while transverse in-plane and out-of-plane resolutions were 1×10^{-5} and 4×10^{-2} Å^{-1}, respectively. The high flux available from the rotating anode source makes it possible to perform high-resolution measurements even of weak reflections. The sample was magnetically aligned by cooling from the isotropic phase in a two-stage oven with a temperature stability and precision of better than ± 10 mK. It should be noted that all the scans were taken during cooling cycles. The sample alignment degraded in lower temperature phases, which made it difficult to perform scans while heating.

Primarily, two types of scans, $q_{\|}$-scans and ω-scans, were performed. During the latter, the detector is fixed at a selected peak position and the intensity of this peak is measured as the sample is rotated through an angle ω about an axis perpendicular to the scattering plane. The $q_{\|}$-scans provide information regarding the smectic layer thickness, while the ω-scans yield an orientational map of smectic layers of known thickness. Two reflections from a single phase, for example, q_0 and $2q_0$ peaks from the S_{A_2} phase originate from the same scattering volume in the sample and their ω-scans should be and *are* identical. Conversely, when the ω-scans of two peaks are different, they either originate from physically different domains, implying a coexistence of two phases or non-collinearity of the corresponding density modulations. The ω-scan is a very powerful tool to determine the coexistence of frustrated smectic phases with two collinear density waves.

Longitudinal (or $q_{\|}$-) scans were conducted to determine the temperature dependence of the layer spacings in different smectic phases. The number of reflections and relationship(s) between their peak positions helped in identifying the phases. The ω-scans of the peaks obtained in longitudinal scans determined whether the reflections originated from the same or different scattering volumes. In addition, mesh scans were performed in the $q_{\|} - q_{\perp}$ plane to check for off-axis peaks which are likely to be present in the $S_{\tilde{A}}$, $S_{A_{crenellated}}$, etc., phases.

6. Recent developments

Application of the high-resolution X-ray technique has revealed new details of frustrated liquid crystalline materials which challenge our current understanding of them. These developments are discussed below.

6.1. *The '$S_{A_{is}}$' phase*

The existence of the $S_{A_{is}}$ phase was reported only in the DB8OCN + 8OBCAB system in a narrow concentration range around 77·2 mol% DB8OCN. Figure 9 (*a*) shows the Bragg peaks and their evolution with temperature in a 76·95 mol% DB8OCN + 23·05 mol% 8OBCAB mixture obtained with the high-resolution technique. The q' peak in the S_{A_d} phase was accompanied by its second harmonic, not visible in this figure, that was lower in intensity by approximately three orders of magnitude. The two quasi-Bragg peaks from the S_{A_2} phase are observed at low temperatures. In the intermediate region, from 144 to 137°C, where the incommensurate phases were reported, peaks corresponding to the S_{A_d}, S_{A_1} and S_{A_2} phases are simultaneously present. As shown in figure 9 (*b*), four quasi-Bragg peaks and one diffuse peak belonging to the S_{A_1} phase are observed in the middle of this region, at 142·55°C. The two $2q_0$ peaks from the S_{A_1} and S_{A_2} phases are resolvable with our high-resolution. Obviously, a single uniform (incommensurate) phase does not exist in this region.

The results of ω-scans taken for the four sharp peaks at 142·53°C are shown in figure 10. The ω-scans for the $2q_0$ and q_0 peaks from the S_{A_2} phase match perfectly, showing that the two reflections originated from the same scattering volume. The ω-scan of this $2q_0$ peak is very different from that of the $2q_0$ peak belonging to the S_{A_1} phase (at nearly the same value of scattering vector) and the q' peak of the S_{A_d} phase. Distinct ω-scans of the four reflections prove that the $S_{A_{is}}$ phase, previously reported in this material, is in fact a coexistence of three smectic phases. The peak intensities in the coexistence region evolved slowly with time, indicating non-equilibrium conditions. This time dependence will be discussed below in greater detail.

6.2. *The '$S_{A_{il}}$' phase*

The $S_{A_{il}}$ phase was previously found to form in the DB8OCN + 8OBCAB mixtures at less than ~77 mol% DB8OCN. The strongest peaks in this region of the phase diagram were at q' and $2q_0$, as expected. Recent measurements, on the other hand have shown that the S_{A_d} and S_{A_1} phases coexist in this region. Figure 11 shows the $q_{\|}$- and ω-scans of these two peaks for a mixture with 73·02 mol% DB8OCN. The difference in the two ω-scans established their coexistence.

In this mixture, coexistence of the S_{A_d} and S_{A_1} phases was observed at the transition between them. In the coexistence region, two diffuse peaks in the proximity of q_0 appear for short periods of time, soon after a change in temperature is effected. These diffuse peaks arise from short-range liquid-like order in regions of ~180–200 Å. Similar

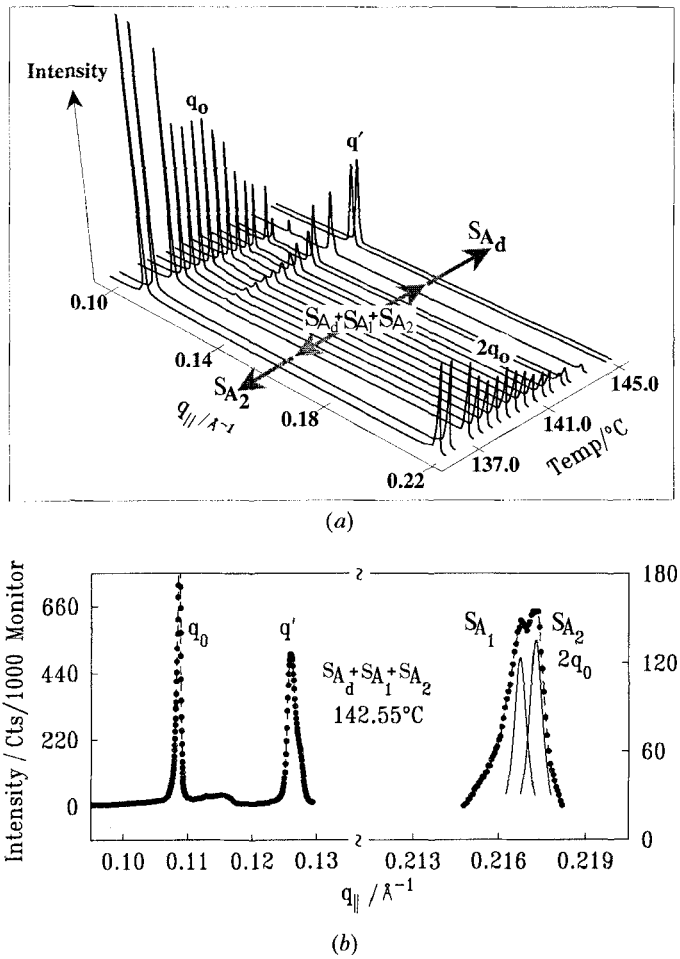

Figure 9. (*a*) Thermal evolution of various X-ray reflections for the 76·95 mol per cent mixture of DB8OCN + 8OBCAB. Reflections from the S_{A_d}, S_{A_1} and S_{A_2} phases are visible in the middle part. (*b*) The longitudinal scan at 142·55°C shows, on a magnified scale, peaks from the three phases.

observations have previously been reported by Fontes *et al.*, at the S_{A_d} to S_{A_1} transition in mixtures of DB5 and T8. It should be pointed out that these diffuse peaks may appear sharp and stable using a low resolution technique and if measurements are made over a short period of a few hours. It was found that at a fixed temperature, these diffuse peaks move towards q_0 and their intensity diminishes with time over a period of seven hours. This is shown with open circles in figure 12. The time dependence, evidently, is due to the fact that the system equilibrates very slowly at these first order phase transitions.

6.3. *The '$S_{A_{i2}}$' phase*

The $S_{A_{i2}}$ phase was reported in both the DB7OCN + 8OCB and DB8OCN + 8OBCAB systems to appear between the S_{A_d} and S_{A_2} phases. We discuss below the results that prove that it is in fact a coexistence of the S_{A_d} and S_{A_2} phases.

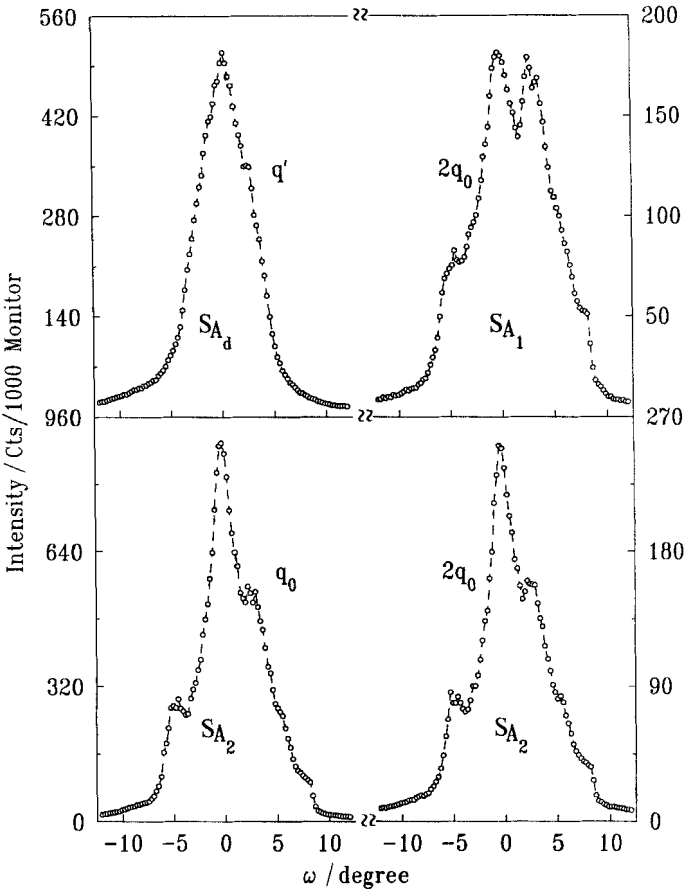

Figure 10. The ω-scans of the S_{A_d}, S_{A_1}, and two S_{A_2} peaks shown in figure 19(*b*) at 142·53°C in the 76·95 mol per cent DB8OCN + 8OBCAB mixture. The mosaicity of each of the two S_{A_2} reflections is identical, but different from that of the S_{A_d} and S_{A_1} reflections, proving the phase coexistence.

The region between 108° and 120°C corresponds to the previously identified incommensurate $S_{A_{i2}}$ phase in a 35·1 mol% 8OCB + 64·9 mol% DB7OCN mixture according to the published phase diagram reproduced in figure 5. In the S_{A_d} phase at 121·35°C, two quasi-Bragg peaks at $q' = 0{\cdot}1328$ and $2q' = 0{\cdot}2656\ \text{Å}^{-1}$, and a diffuse peak at $2q_0 \sim 0{\cdot}2389\ \text{Å}^{-1}$ were observed as shown in figure 13(*a*). ω-scans at this temperature revealed a well-aligned sample with half-width of $\sim 2{\cdot}3$ degrees. The ω-scans of the two S_{A_d} peaks (see figure 13(*b*)) were identical, confirming that both reflections originated from the same scattering volume of the sample and that the corresponding mass density modulations were collinear.

At temperatures lower than 120°C, two additional sharp peaks corresponding to the underlying S_{A_2} phase appeared at $q_0 = 0{\cdot}1211$ and $2q_0 = 0{\cdot}2422\ \text{Å}^{-1}$. These peaks gradually became stronger, and at 119·35°C, their intensities became comparable to the peaks at q' and $2q'$. The four peaks were present at all temperatures above 108°C, although their relative intensities varied with temperature and slowly with time (to be discussed later). Figure 14 shows the four peaks at 115·69°C. Since the $S_{A_{i2}}$ phase is expected and previously found to have three reflections at q', q_0 and $2q_0$ the simultaneous presence of four peaks suggested a coexistence of S_{A_d} and S_{A_2} phases.

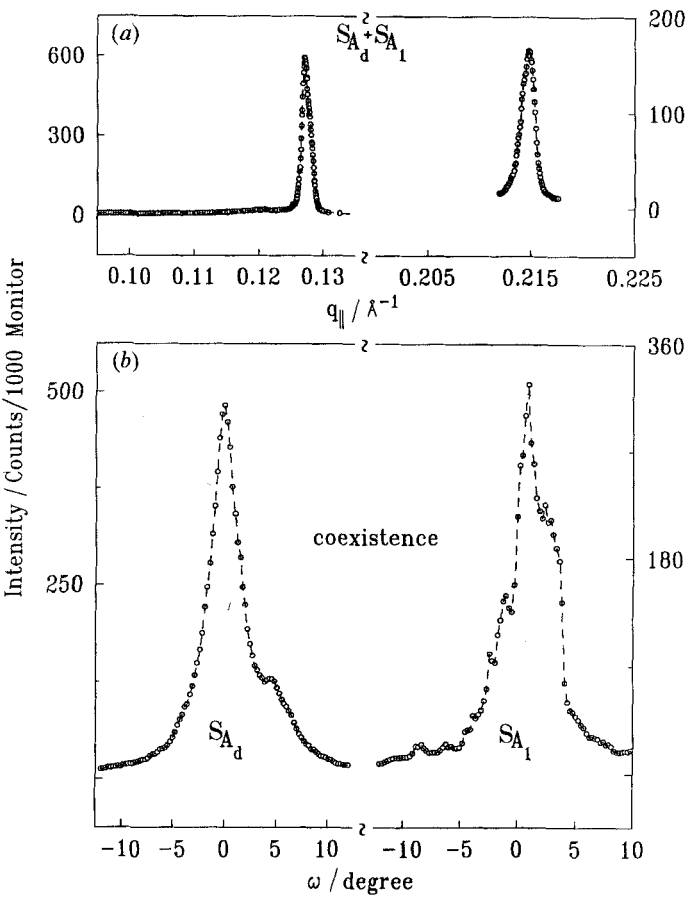

Figure 11. (*a*) Longitudinal, and (*b*) ω-scans taken at 137·92°C for the 73·02 mol per cent DB8OCN + 8OBCAB mixture. The ω-scan of the S_{A_d} peak is different from that of the S_{A_1} peak, proving the coexistence of the two phases.

The shapes of ω-scans taken through the two S_{A_d} peaks at 119·35°C were similar to each other as shown in the uppper part of figure 14 (*b*). The ω-scans of the two S_{A_2} reflections (see figure 14 (*b*), lower panel) were also identical, but quite different from those of S_{A_d} peaks. Longer counting times were used for the peaks at $2q_0$ and $2q'$ because of their low intensity. This resulted in different backgrounds for the q_0 and q' peaks. Also, the scans were taken at different times while the sample mosaic was changing. These two factors were responsible for minor differences in the curves shown in figure 14 (*b*). The half-width of the ω-scans of S_{A_d} reflections was approximately 4·7°, while that of S_{A_2} peaks was nearly 7·2°. The ω-scans for all Bragg reflections from a $S_{A_{12}}$ phase should have been identical. These observations proved that smectic density wave-vectors corresponding to the S_{A_d} and S_{A_2} phases were not only non-collinear, but also originated from different parts (domains) of the sample.

The peaks at q_0 and $2q_0$ became more intense, while those at q' and $2q'$ grew weaker at lower temperatures and eventually disappeared at approximately 108°C. The ω-scans through the two S_{A_2} peaks at 105·22°C were, again, identical suggesting that they originated from two collinear density modulations.

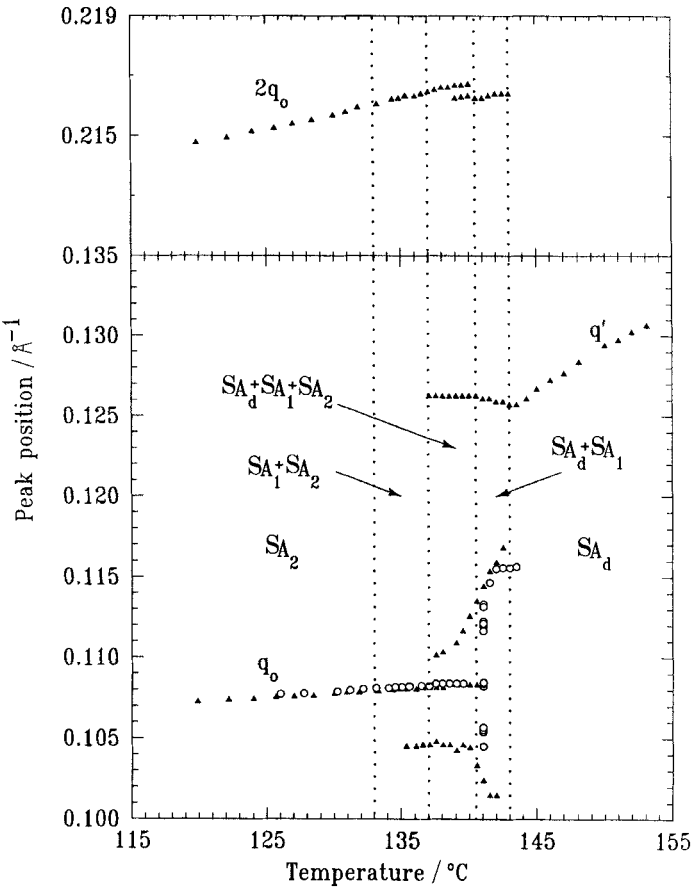

Figure 12. Temperature dependence of peak positions for various phases of the 76·07 mol per cent DB8OCN + 8OBCAB mixture. Open circles were obtained during a repeat scan. The points at 141·0°C represent the time evolution of the two diffuse peaks which finally collapse onto the q_0 peak after ~ 7 h due to slow equilibration.

The cause of the observed coexistence was slow equilibration at the first order transitions between the respective smectic phases. Upon cooling the sample from the S_{A_d} phase to a point in the middle of the coexistence region, the peak intensities were found to change with time. For example, the intensity of the S_{A_d} peak 4 K below the S_{A_d} phase of the 35·1 mol% 8OCB + DB7OCN mixture dropped simultaneously with an exponential increase in the S_{A_2} peak intensity with a time constant of approximately 12·4 h (see figure 15). As a consequence of slow relaxation, equilibrium measurements became almost impossible to make. Other hallmarks of coexistence, such as concentration changes accompanying the phase separation, were also observed experimentally in subsequent cooling cycles. Concentration changes manifest themselves as changes in the smectic layer spacing and consequently in the values of the scattering vectors of the same reflections.

Independent NMR evidence for a biphasic region in a mixture of 65 mol% DB7OCN + 35 mol% 8OCB-*d*2 (deuteriated in the alkyl chain at the site closest to the benzene ring) was obtained by Ukleja *et al.* [22]. Inset (*a*) in figure 16 shows the deuterium NMR spectrum (100 kHz from left to right) in the S_{A_d} phase just above the

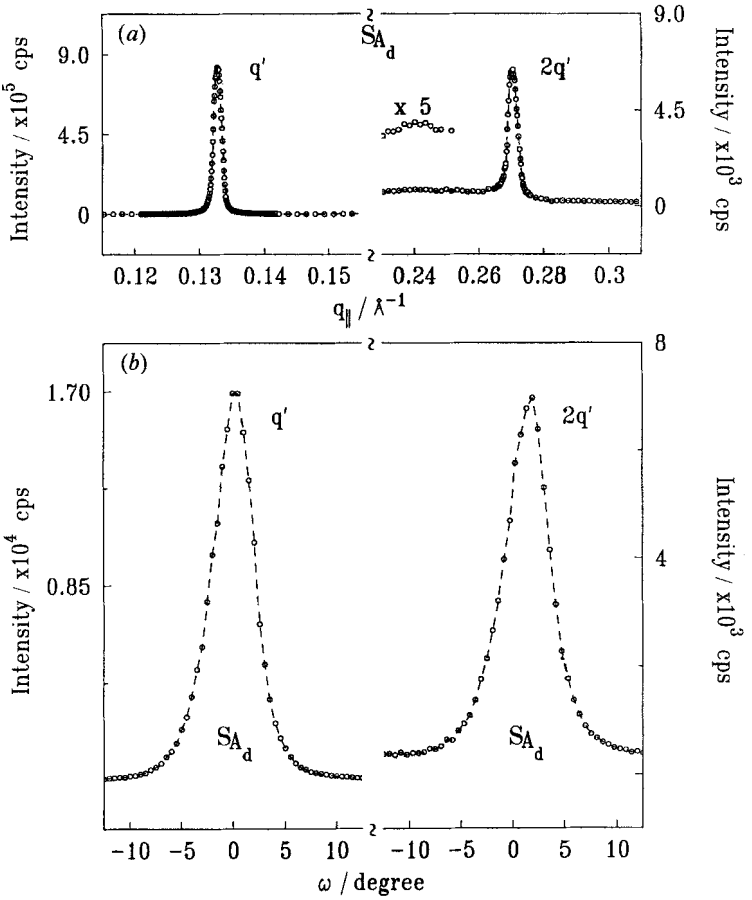

Figure 13 (*a*) A representative $q_\parallel$-scan in the S_{A_d} phase, and (*b*) two identical ω-scans through the S_{A_d} peaks at 121·35°C for the 35·1 mol% 8OCB + DB7OCN mixture.

region previously attributed to the $S_{A_{i2}}$ phase. The appearance of this doublet indicates a sample with a well-aligned director. The spectrum (*b*) in figure 1 (*b*) was taken after the sample was cooled by 10 K into the '$S_{A_{i2}}$' region. It shows a second doublet with a splitting about 10 per cent larger than the first. As the temperature is lowered, the intensity of the outer pair increases at the expense of the inner pair. This behaviour shows the existence of two molecular environments of the deuterium nuclei and is consistent with a phase separation into two components, one in the S_{A_d} phase, and the other in the S_{A_2} phase. The graph shows the splittings as a function of temperature (cooling). The existence of two sets of doublets implies that 8OCB molecules do not sample both molecular environments during the time of the evolution of the NMR signal, several hundred microseconds. This suggests that the S_{A_d} and S_{A_2} domains are at least several tenths of microns across (assuming a diffusion coefficient of ~ 10–$11\ m^2 s^{-1}$), or that there is very strongly restricted diffusion at boundaries between the regions. On the other hand, the samples very quickly reverted to the single pair of doublets when heated to the S_{A_d} phase, which argues that complete bulk demixing occurs over periods much longer than the time (several hours) that it takes to complete these measurements.

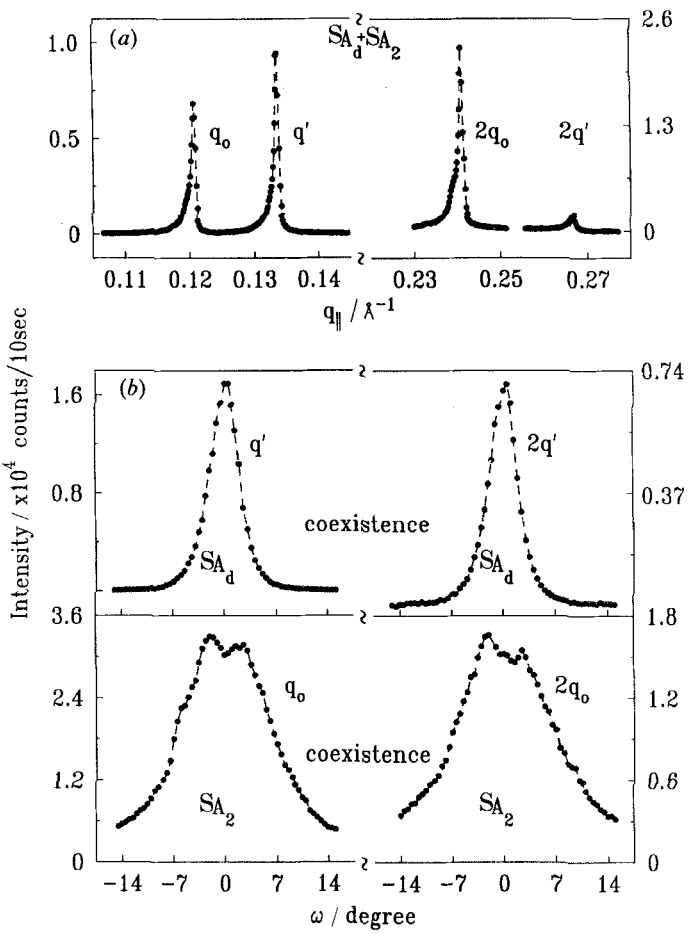

Figure 14 (*a*) A representative longitudinal ($q_\parallel$-) scan in the coexistence region at 115·69°C and (*b*) ω-scans at 119·35°C in a 35·1 mol% 8OCB + DB7OCN mixture. The mosaic scans of the two S_{A_d} reflections are identical, but different from those of the S_{A_2} peaks.

6.4. *The S_{A_d} to S_{A_2} phase transition*

The S_{A_d} and S_{A_2} phases were found to coexist over a finite temperature range for concentrations ranging from zero to 35·1 mol% 8OCB. This coexistence was easy to infer from the simultaneous presence of reflections from the two phases for mixtures with concentrations above 14 mol%. At concentrations below 14 mol% however, the q_0 and q' peaks were not resolved and, therefore, it became impractical to obtain their ω-scans. The intensity of the q_0 peak, which appeared to evolve into the q' peak, was found to drop and its width broaden near the S_{A_d} to S_{A_2} transition. The peak became narrow after the transition to the S_{A_2} phase was complete. We interpret this effect as being due to the simultaneous presence of the q_0 and q' peaks, evidently due to coexistence.

In this system, coexistence of the S_{A_d} and S_{A_2} phases extends from zero to nearly 40 mol% 8OCB. The critical point on the S_{A_d} to S_{A_2} transition line is projected to be at a negative 8OCB concentration. The temperature dependence of the smectic wave-

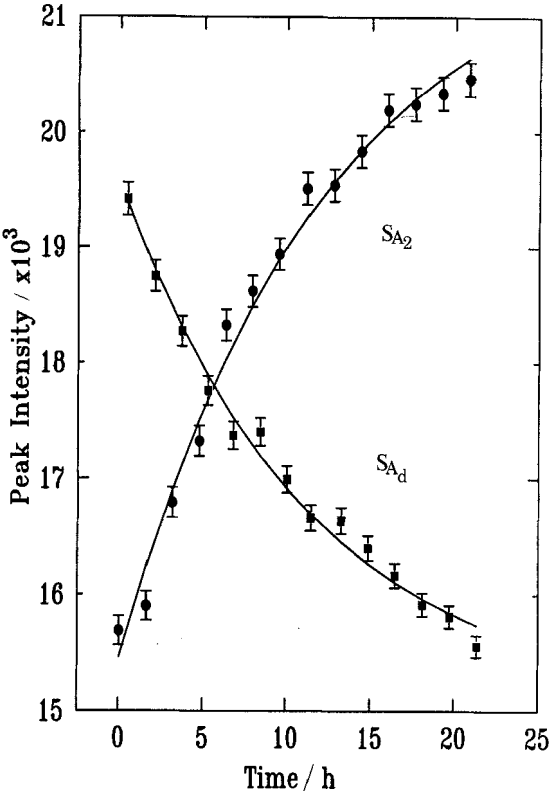

Figure 15. Time dependence of the peak intensities at $q_0 = 0{\cdot}1206\,\text{Å}^{-1}$ of the S_{A_2} phase and $q' = 0{\cdot}1336\,\text{Å}^{-1}$ of the S_{A_d} phase (different vertical scales) at 116·36°C in the coexistence region after the sample is cooled from the S_{A_d} phase. The solid lines represent exponential fits, both with a time constant of approximately 12·4 h.

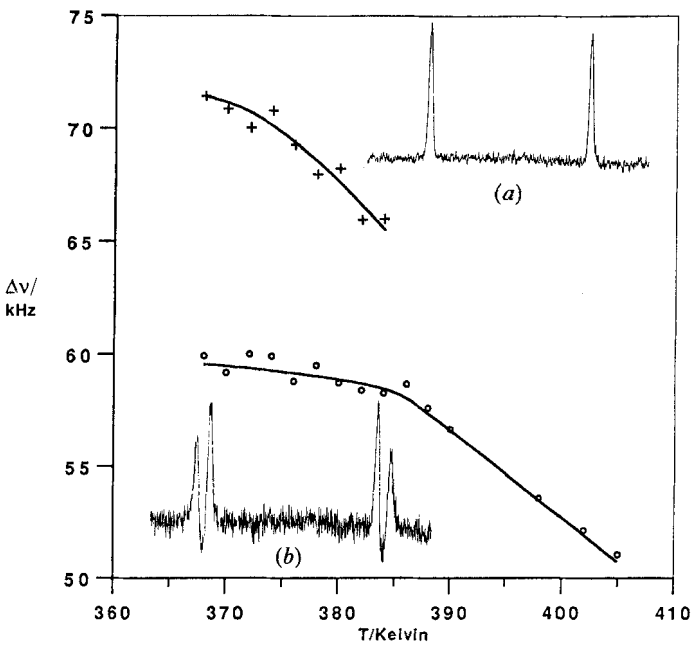

Figure 16. Deuterium NMR spectra and quadrupolar splittings versus temperature for the mixture of 65 mol% DB7OCN + 35 mol% 8OCB-*d*2. Inset (*a*) shows the spectrum upon cooling an aligned sample to 390 K. Inset (*b*) shows the spectrum upon cooling to 380 K. Both show a region of 100 kHz.

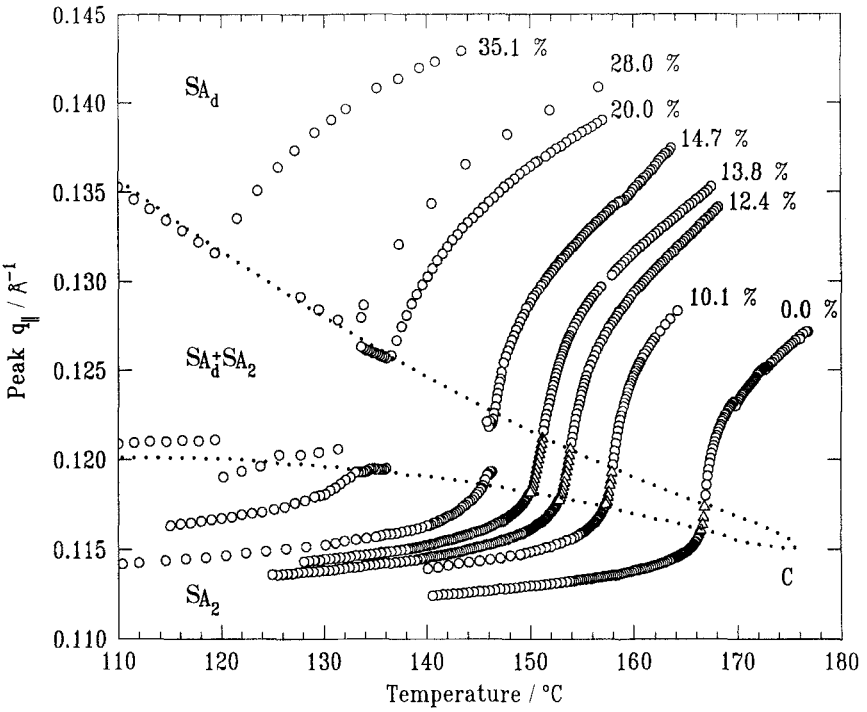

Figure 17. Temperature dependence of the wavevectors, q' in the S_{A_d} phase and q_0 in the S_{A_2} phase for eight different concentrations of 8OCB. The two peaks are resolved over a finite temperature range for concentrations higher than 14 mol%. At concentrations below 14 mol%, a dramatic increase in peak width and an associated drop in peak intensity are used to infer the coexistence (triangles) as discussed in the text. The dotted line is drawn to represent approximately the coexistence region.

vectors q_0 and q' is shown in figure 17, for different compositions in the proximity of this critical point. It exhibits a remarkable resemblance to the liquid-gas phase diagram, in accordance with theory [3].

The S_{A_d}, S_{A_2} coexistence curve (figure 18) of the second system is very similar to that of the DB7OCN + 8OCB system. The width of the coexistence region decreases with increasing concentration of DB8OCN and eventually appears to terminate at a critical point. One quantitative difference between the two systems is that in the DB8OCN + 8OBCAB system, the modulation q_0 of the S_{A_2} phase is essentially independent of the concentration.

6.5. *Phase diagrams of 8OBCAB + DB8OCN and 8OCB + DB7OCN systems*

The experimentally observed coexistence in the 8OBCAB + DB8OCN system has firmly established the strongly first order nature of the S_{A_d}–S_{A_1}, S_{A_d}–S_{A_2}, and S_{A_1}–S_{A_2} phase transitions represented by solid lines (in figure 19) through the coexistence regions. Figure 19 (*a*) thus represents the correct experimental phase diagram of this system. The inset in figure 19 (*a*) shows the details of the phase coexistence in the proximity of 77 mol% concentration. The transition temperatures obtained in our study are slightly higher than those shown [18] in figure 7, due to higher sample purity. The theoretically calculated phase diagram [3] originally plotted in terms of

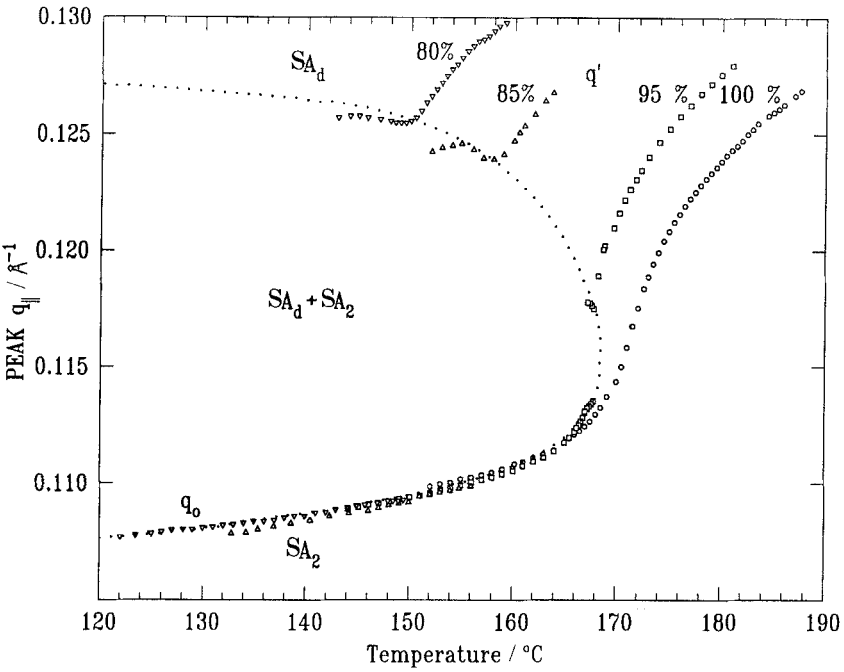

Figure 18. Temperature dependence of scattering vectors in the S_{A_d} and S_{A_2} phases for four different concentrations of DB8OCN in DB8OCN + 8OBCAB mixtures. The dotted line represents the outline of the $S_{A_d} + S_{A_2}$ coexistence region.

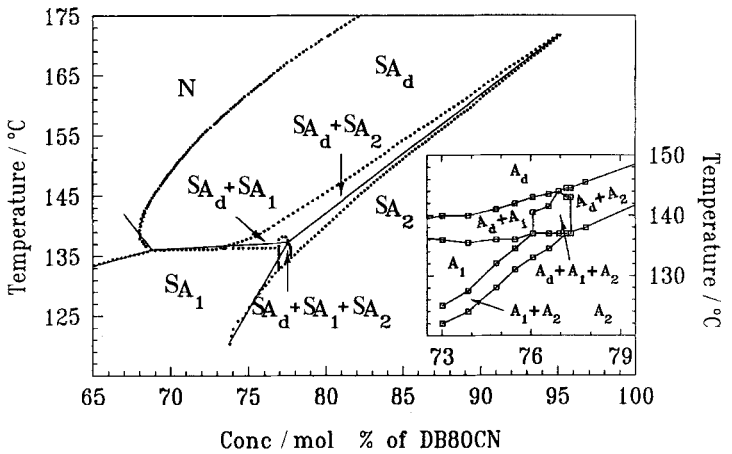

(*a*)

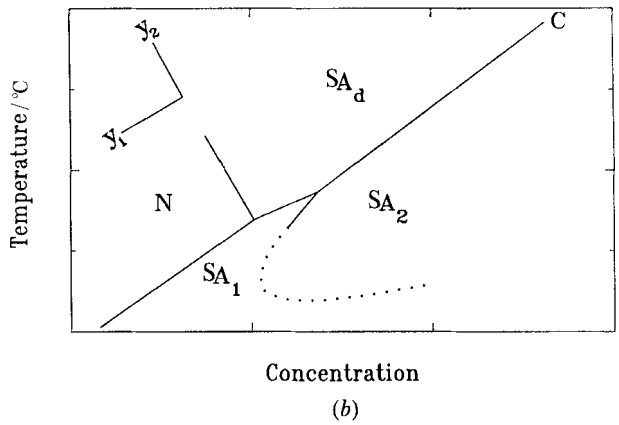

Figure 19. (*a*) Experimental phase diagram (dotted lines) of the DB8OCN + 8OBCAB system (from [18]). Solid lines represent first order transitions. The inset shows the partial phase diagram based on results of the present study. (*b*) The theoretical phase diagram from [3] is replotted after a rotation by $\sim 122°$ to generate the temperature–concentration phase diagram.

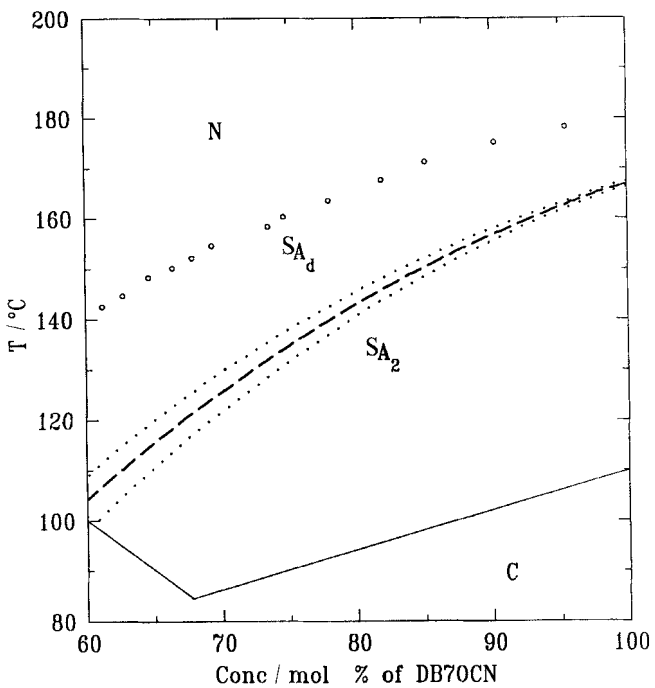

Figure 20. The phase diagram of the 8OCB + DB7OCN system replotted with the DB7OCN concentration along the abscissa. The dotted curves approximately define the boundaries of the S_{A_d} to S_{A_2} coexistence and the dashed line in this region represents the first order S_{A_d} to S_{A_2} transition.

parameters, y_1 and y_2, that are linear functions of temperature and concentration is reproduced in figure 19(*b*). Its axes have been rotated to transform it into the concentration–temperature space, to facilitate a comparison with the experimental phase diagram. Theory and experiments are in excellent agreement, as evident from the similar topology of the two phase diagrams. The phase diagram of the DB7OCN + 8OCB systems (see figure 5), when replotted with DB7OCN concentration along the horizontal axis (figure 20), also has the same topology as the upper part of the theoretical phase diagram (figure 19(*b*)).

7. Summary

The results discussed above leave us with no known system that exhibits incommensurate smectic A phases. However, the results do not in any way rule out the possibility of their existence in other more suitable materials. There is a need to take a fresh look and conduct well-coordinated theoretical investigations and experimental search of these intriguing phases.

The authors have greatly benefited from conversations with T. C. Lubensky, J. Prost, C. W. Garland, D. L. Johnson, R. Shashidhar, and P. A. Heiney. The NMR facilities were kindly provided by N. Boden at the University of Leeds. This work was supported by the National Science Foundation under grant DMR-89-20147. Materials were provided by M. E. Neubert and S. Keast under NSF-DMR-88-18561.

References

[1] SIGAUD, G., HARDOUIN, F., ACHARD, M. F., and GASPAROUX, H., 1979, *J. Phys., Paris, Colloq.*, **40,** C3-356.
[2] GARLAND, C. W., 1990, *Geometry and Thermodynamics*, edited by J. C. Toledano (Plenum Press), p. 221.
[3] BAROIS, P., PROST, J., and LUBENSKY, T. C., 1985, *J. Phys., Paris*, **46,** 391.
[4] PROST, J, 1984, *Adv. Phys.*, **33,** 1 and references therein.
[5] WANG, J., and LUBENSKY, T. C., 1984, *Phys. Rev.* A, **29,** 2210.
[6] LUBENSKY, T. C., RAMASWAMY, S., and TONER, J., 1988, *Phys. Rev.* A, **38,** 4284.
[7] WANG, J., and LUBENSKY, T. C., 1983, *J. Phys., Paris*, **45,** 1653.
[8] BAROIS, P., COULON, C., and PROST, J., 1981, *J. Phys., Paris, Lett.*, **42,** L-107.
[9] PROST, J., and BAROIS, P., 1983, *J. Chim. phys.*, **80,** 65.
[10] BAROIS, P., POMMIER, J., and PROST, J., 1992, *Solitons in Liquid Crystals*, edited by L. Lam and J. Prost (Springer-Verlag), p. 191.
[11] BROWNSEY, G. J., and LEADBETTER, A. J., 1980, *Phys. Rev. Lett.*, **44,** 1608.
[12] RATNA, B. R., SHASHIDHAR, R., and RAJA, V. N., 1985, *Phys. Rev. Lett.*, **55,** 1476.
[13] GARLAND, C. W., and DAS, P., 1987, *Incommensurate Crystals, Liquid Crystals, and Quasi Crystals*, edited by J. F. Scott and N. A. Clark (Plenum), p. 297.
[14] DAS, P., EMA, K., GARLAND, C. W., and SHASHIDHAR, R., 1989, *Liq. Crystals*, **4,** 581.
[15] BAROIS, P., 1986, *Phys. Rev.* A, **33,** 3632.
[16] FONTES, E., HEINEY, P. A., BAROIS, P., and LEVELUT, A. M., 1988, *Phys. Rev. Lett.*, **60,** 1138; FONTES, E., LEE, W. K., HEINEY, P. A., NOUNESIS, G., GARLAND, C. W., RIERA, A., MCCAULEY, J. P., and SMITH, A. B., 1990, *J. chem. Phys.*, **92,** 3917.
[17] A different notation, q_0' instead of q', was used in this paper.
[18] SHASHIDHAR, R., and RATNA, B. R., 1989, *Liq. Crystals*, **5,** 421.
[19] KUMAR, S., CHEN, L., and SURENDRANATH, V., 1991, *Phys. Rev. Lett.*, **67,** 322.
[20] PATEL, P., KEAST, S., NEUBERT, M. E., and KUMAR, S., 1992, *Phys. Rev. Lett.*, **69,** 301.
[21] PATEL, P., CHEN, L., and KUMAR, S., 1993, *Phys. Rev.* E, **47,** 2643; PATEL, P., and KUMAR, S., 1993, *Europhysics Lett.*, **23,** 135.
[22] UKLEJA, P., *et al.* (to be published).